Journal of Physics: Conference Series **194** (2009) 012056 doi:10.1088/1742-6596/194/1/012056

Two-particle emission from LiF(1 0 0) upon photon, electron and positron excitation

GA van Riessen, FO Schumann, M Birke, C Winkler and J Kirschner

E-mail: riessen@mpi-halle.mpg.de
Max-Planck Institute of Microstructure Physics, Weinberg 2, 06120 Halle, Germany

Abstract.
Electron pairs simultaneously emitted from a solid surface upon excitation with photons (double photoemission or (γ, 2e)) or electrons (e,2e) provide information about the electron correlation in the solid which is mediated by exchange and Coulomb interactions. Without the Pauli restriction, the correlation of a positron with many electrons in a solid is dominated by Coulomb interactions. We have therefore undertaken the first comparative study of electron-electron and positron-electron pair emission upon impact with low energy photons, electrons and positrons. The target surface chosen for this study was LiF(1 0 0), a wide band gap dielectric that allows for a simple kinematical interpretation of the energy distribution of emitted pairs. We present the first results and discuss insights into the mechanisms of pair emission upon positron, electron and photon impact.

1. Introduction

It was recently demonstrated that correlated positron-electron pairs are emitted from a LiF(1 0 0) surface upon excitation with a low energy positron beam [1], making available a new reaction channel to compliment those established for electron and photon stimulated pair emission, namely (e,2e) and (γ, 2e) (or double photoemission (DPE)). Such multi-particle coincidence experiments from solid surfaces provide a sensitive probe of electron-electron correlation that underlies phenomena such as magnetism and superconductivity and which continues to present a formidable challenge to theory. A concept central to electron correlation in condensed matter is that of the exchange-correlation (xc)-hole which can be described as a depletion of the average electron density around an individual electron due to mutual Coulomb and exchange interactions with other electrons (see, e.g., refs. [2, 3, 4]). Its extent in momentum space is a measure of the pair-correlation function which is a central quantity in the theory of many-body systems.

Experimental challenges, including the inherently small probability of detecting two *correlated* electrons produced during a single scattering process, were overcome to demonstrate that information about the correlation between a pair of electrons in the solid can be recovered from the observed momenta of the pair of electrons emitted from the surface upon photon or electron impact [5, 6, 7, 8, 9, 10, 11, 12]. Moreover, it

has been shown that with $e^- - e^-$ pair emission spectroscopy it is possible to directly probe the xc-hole [5, 7].

The interaction between positrons and electrons is essentially Coulombic, without the exchange effects characteristic of the interaction between indistinguishable electrons. It follows that by employing a low energy positron beam and observing correlated $e^+ - e^-$ pairs emitted from a surface after their interaction in the solid may provide a route by which the role of the (attractive) Coulomb interactions can be probed without direct influence of exchange interactions. The development of low energy e^+ beams of high brightness in recent years has lead to resurgent interest in e^+-surface interaction. A detailed understanding of $e^+ - e^-$ correlation is essential for interpretation of e^+ annihilation based measurements that provide a sensitive probe to the electronic structure of solids [13]. Despite considerable theoretical investigation, there remains some unexplained discrepancies between theory and experiment, even for simple metals [14, 15]. The (e^+,e^+e^-) reaction channel, which may provide new insight into the problem, exploits the fact that scattering of positrons back to the vacuum from a surface occurs with significant probability with respect to competing processes such as annihilation and positronium formation (see, e.g. Ref. [16]).

Berakdar [17], and more recently Giebels *et al* [18] have studied $e^+ - e^-$ pair emission from solid surfaces and shown that distinguishability of the e^- and e^+ leads to differences between the momentum distribution of $e^+ - e^-$ pair emission upon e^+ impact and $e^- - e^-$ pair emission upon e^- impact. Giebels *et al* considered a Cu(1 1 1) surface for which e^--solid and e^+-solid interactions potential were obtained by density functional theory, multiple scattering was properly described, and $e^+ - e^-$ correlation in the final two-particle state was represented by a product of a low energy electron (positron) diffraction states coupled by a screened Coulomb interaction. Comparison with spin-unresolved (e,2e) angular distributions revealed differences that could be attributed to exchange. Comparison to (e,2e) angular distributions for two electrons of opposite spins also revealed, despite the absence of exchange, distinct differences that were attributed to the single-particle e^+-solid and e^--solid potentials containing attractive and repulsive correlation parts, respectively, and a stronger Coulomb correlation between the e^+ and e^- than between two electrons. Giebels *et al* obtained $e^- - e^-$ and $e^+ - e^-$ pair correlation functions that describe the probability of finding one particle at $\mathbf{r_1}$ in the vicinity of the other at $\mathbf{r_2}$. At $\mathbf{r_1} = \mathbf{r_2}$ there is, as expected, a minimum for an $e^- - e^-$ pair, i.e., a correlation hole reflecting the tendency for electrons to avoid each other, and a maximum for a $e^+ - e^-$ pair, i.e. a correlation hill. Qualitatively, the depth (height) of the correlation hole (hill) reflects the difference in correlation energy that can be understood in terms of the probability of finding two electrons at the same location, which can not be less than zero, and the probability of finding a e^+ and an e^- at the same location, which has no obvious upper limit due to the absence of exchange [18].

Comparison between two-electron emission spectra obtained with photons and electrons is of interest because of the distinctive differences in their mechanism of excitation, momentum transfer and propagation in the crystal. Direct double photoemission, a process forbidden in the absence of correlation between two electrons in the initial state [10], has been recognized in DPE from metallic surfaces [19, 20] through manifestation of the so-called propensity rule [10]. The validity of the propensity role and the role of the indirect process of pair emission preceded by single-photoemission is an area of continued investigation for which comparison of DPE spectra to (e,2e) spectra has been shown to be useful [21].

In this article we present new double photoemission data from a LiF(1 0 0) surface and compare it to the previously reported (e^+,e^+e^-), (e^+,e^-e^-) and (e^-,e^-e^-) data [1] obtained under similar conditions with the same apparatus.

2. Experiment

The experiment essentially consisted of the detection of $e^- - e^-$ or $e^+ - e^-$ pairs emitted upon impact with electrons, positrons or photons incident upon a LiF(1 0 0) crystal in an arrangement illustrated in Figure 1. All measurements were performed in reflection geometry with the primary beam oriented along the surface normal and electron-optical axes of two analyzer input lenses positioned at 45° from the surface normal. The 200 mm electrostatic hemispherical analyzers (Scienta R4000) with spatially resolving detectors (multichannel plates (MCP) and resistive anodes) were employed to detect positrons and electrons and to record angle-integrated energy spectra. Either positrons or electrons could be analyzed by reversing the polarity of potentials applied to the relevant optical elements. The analyzers, sample and positron optics were mounted in a UHV chamber. The time interval between the detection of a particle on one detector and the arrival of a second particle on the other detector was measured using signals originating from the MCP. The measured interval is used to distinguish correlated particles emitted during a single process (true coincidences) from those that involve the detection of two unrelated particles produced by separate ionization events that fortuitously arrive together at the detectors (accidental coincidences). True coincidences are always observed within a time interval given by the experimental time resolution and the random coincidences are uniformly distributed in time.

The sample was a LiF(1 0 0) crystal cleaned by heating to 450° Celsius. During measurements the crystal temperature was 150° Celsius to minimize contamination and to mitigate electrostatic charging of the surface.

The source of electrons for (e,2e) measurements was a standard focused e^- gun with a BaO cathode. The source of the moderated 85 eV e^+ beam was the neutron induced e^+ source (NEPOMUC) [22] at the FRM-II reactor. The moderated beam was magnetically guided along the beamline in a 10 mT longitudinal magnetic field until it was extracted through an aperture in magnetically conductive iron shield and electrostatically focused to a 1 mm spot at the target. Further experimental details are available elsewhere [1, 23] The primary e^+ flux was estimated to be 5×10^4 s^{-1} from the rate of e^+ annihilation at the sample. For $(\gamma, 2e)$ experiments, the source of linearly polarized light was the UE56/2-PGM-1 beamline at BESSY II [24]. To maintain an acceptable ratio of true-accidental coincidences additional apertures were placed in the beam with a diameter down to 30 μm.

The analyzer transfer lenses were operated in a mode optimized for high transmission of low kinetic energy electrons or positrons, integrating over an angular range of approximately ±15° about the scattering plane. An energy range of approximately ±5% of the pass energy (300 eV) was measured simultaneously. With e^- beam experiments the lenses and analyzers were configured to accept charged particles with a mean kinetic energy of 35 eV, for e^+ beam experiments 30 eV. For $(\gamma, 2e)$ experiments a photon energy of 128 eV was chosen to avoid overlapping core-hole excitations and accordingly the mean kinetic energy of detected electrons was set to 51 eV. The total energy resolution for e^-, and e^+ experiments, including the beam energy spread, were estimated from the energy width of the elastically scattered peak to be 0.46 eV and 4 eV, respectively. For photon excited experiments

the energy resolution was estimated to be 0.7 eV from the measured width of the Li 1s photoelectron peak. Data were acquired for (e^-,e^-e^-), (e^+,e^+e^-), (e^+,e^-e^-) and (γ,e^-e^-) reactions for a total of 90, 62, 11, and 106 hours, respectively.

3. Results

Figure 1 shows the measured energy distribution of e^-−e^- pair emission upon e^- excitation, e^+−e^- emission upon e^+ excitation, and two-electron photoemission from LiF(1 0 0). For a given position on the two-dimensional energy spectra, the energies of the two detected coincident particles, E_1 and E_2, are given by its coordinates and the number of events detected for that particular combination of energies is represented by the color. Also shown are projections onto the line $E_1 = E_2$ for events for which $|E_1 - E_2| < 7$ eV. This projection represents the sum kinetic energy $(E_1 + E_2)$ distribution of correlated pairs of particles.

In the case of DPE the ratio of true-to-accidental coincidences was relatively low (≈ 1) so to better reveal the correlated e^- distribution the intensity of accidental coincidences has been subtracted from the intensity of the true coincidences at each point. Both quantities are measured simultaneously and, as described above, distinguished on the basis of the arrival time between a pair of particles. With e^- and e^+ excitation the true-to-accidental (T/A) ratio was, respectively, about 7 and 20 and the accidental fraction has not been subtracted. The differences in T/A ratio are dominated by the differences in primary particle or photon flux.

Energetic correlation between detected particles is evident in the energy distributions for all excitation sources as a distinctive ridge of intensity parallel to a line of constant sum kinetic energy of the detected particles, $E_s = E_1 + E_2$. We emphasize that no corresponding spectral structure is present in the accidental energy distribution (not shown). In the absence of further scattering processes, E_s is conserved when two particles are emitted together by a single process. It also has an upper bound that coincides with the threshold for the emission of the two detected particles, labeled as $E^+_{\rm max}$ in Figure 1. For further discussion of the energetics, instead of considering the total kinetic energy of the pair on the projection axes for Figure 1, we define a binding energy for two emitted particles in an analogous fashion as in conventional photoemission. For DPE, the two-particle binding energy E_{2p} is given by $E_{2p}^{\rm DPE} = h\nu-(E_1+E_2)-2\phi_-$, where ϕ_- is the e^- work function, and $h\nu$ the photon energy. A consistent definition for e^- and e^+ excitation is $E_{2p}^{\rm e,2e} = E_i-(E_1+E_2)-\phi_-$ and $E_{2p}^{\rm p,pe} = E_i^+-(E_1+E_2^+)-\phi_-$. As the top of the unoccupied band in LiF is close to the vacuum level, the e^- work function is nearly equal to the band gap energy, i.e. $\phi_- \sim E_g = 13.0 \pm 0.4$ eV [8].

The onset for pair emission by (e^-,e^-e^-) and (e^+,e^-e^-) occurs for $E_1 + E_2 = E_i - \phi_-$, and by DPE for $E_1 + E_2 = h\nu - 2\phi_-$, corresponding to a final state where the initially bound electron(s) have been ejected into the vacuum from the highest occupied level. Figure 2 shows a comparison of the projections in Figure 1 as two-particle binding energy distributions, on which scale the onset is at zero. The distribution of correlated e^-−e^- pairs emitted upon e^+ impact are also shown in Figure 2. In contrast to the (e^+,e^+e^-) pair energy distribution, no onset at the zero two-particle binding energy is observed. Instead, correlated pair emission intensity increases continuously from $-\phi_-$ downwards, as expected on the basis that two electrons must overcome the work-function to be emitted and the undetected e^+ may

scatter into a continuum of states.

The observed FWHM of the peak in the (e^-,e^-e^-) sum energy spectrum (Figure 2) is 3 eV which closely matches the width of the intense part of the LiF valence band density of states, included for comparison in Figure 2. Both bulk and layer resolved densities of states [25] are included. For DPE the width of the peak in the two-particle binding energy distribution is approximately double because both detected electrons come from the LiF valence band. The wide band gap of LiF prohibits the particles participating in the pair emission processes from losing a continuous range of energy by electronic excitations below E_g (indicated in Figures 1 and 2). Consequently there is a region of low inelastic contributions in the (e,2e), (e^+,e^+e^-) and DPE distributions below the elastic feature. From an energy of E_g below the onset for pair emission the intensity in the distribution increases, reflecting that the pair emission process is accompanied by secondary electronic excitation. Differences in the e^- excited e^-−e^- and e^+−e^- pair distributions in the low energy (inelastic) region may arise from differences in the inelastic scattering cross-sections for positrons and electrons. The low cross-section for elastic back-scattering (diffraction) of the primary e^+ beam at the chosen energy may also account for the relatively small peak in the two-particle binding energy distribution relative to the intensity in the inelastic region. The Bragg peak intensity for a e^+ beam with energy close to that of our primary beam has been reported to be only about 0.1% of the primary intensity [16].

Returning to the two-dimensional energy distributions (Figure 1), we see that the energy distributions are essentially symmetric about the line $E_1 = E_2$ which reflects the symmetric geometry of the experiment (for (e,2e) and DPE). In the case of positron-excited e^+−e^- pair emission the symmetry is broken because the two particles are different. It is therefore expected that asymmetry with respect to the line $E_1 = E_2^+$ in the energy distribution will arise from differences in the energy dependent interactions of the final-state e^- and e^+ with the crystal. This is was recently illustrated by a theoretical investigation (e^+,e^+e^-) from Cu(1 1 1), although only weak asymmetry in the energy distribution was found [18], The limited energy resolution and counting statistics of the present data preclude any detailed analysis of the e^+−e^- energy distribution asymmetry.

Intensity variations along lines perpendicular to $E_1 = E_2$ provide information about how energy is distributed between the two detected particles. In this context we recall a propensity rule for DPE that that the pair intensity is suppressed if the vector sum of the momenta of the emitted electrons is perpendicular to the polarization vector of the light. Hence, in the present geometry with the polarization vector in the scattering plane the emission of electrons of equal energy ($E_1 = E_2$) should be suppressed [10]. In contrast, the DPE data from LiF(1 0 0) show an apparent preference for the emitted electrons to share the energy equally. It should be noted that the distribution has not been corrected for the influence of energy-dependent variations in the coincident detection efficiency, but the tendency to share energy equally is characteristic of indirect double-photoemission, i.e., photoelectron excited e^-−e^- pair emission. The similarity between the DPE and (e^-,e^-e^-) data support such an interpretation. Further, strong differences between spectra obtained when the polarization vector is rotated to be perpendicular to the scattering plane are predicted by the propensity rule. In order to test this prediction, spectra were obtained with two orthogonal orientations of the light polarization vector in an analogous fashion to a recent study of DPE from Cu(1 1 1) [20]. No significant differences were observed

between the two spectra and the data presented are the sum of both measurements. We also note that the validity of the propensity rule has been shown to deteriorate at high DPE energy [26]. The extent to which the propensity rule applies for DPE from solids requires further investigation.

4. Concluding Remarks

We have measured with the same apparatus the energy distribution of correlated e^-−e^- and e^+−e^- pairs emitted from a LiF(1 0 0) surface upon low energy photon, electron, and positron excitation. DPE, (e^-,e^-e^-) and (e^+,e^-e^-) processes have been shown to occur at the energy threshold expected by consideration of the valence electron band structure and with the spectral characteristic of energy-correlation between the detected particles. The width of the structure in the particle sum kinetic energy spectrum reflects the LiF(1 0 0) electron valence band structure. The sharing of energy between the particles of a pair is essentially similar for all excitation sources within the present resolution and statistical limits which is unexpected on account of the asymmetry in the (e^+,e^+e^-) experiment and the propensity rule in the case of DPE. The observation of correlated e^+−e^- emission from LiF(1 0 0) is the first of its kind and demonstrates that the e^+−e^- emission process is sufficiently intense to undertake momentum resolved measurements. Together with the recent extension of a theoretical framework for (e^-,e^-e^-) to (e^+,e^+e^-) [18], this will allow to disentangle the contributions of exchange interaction and Coulomb correlation by detailed comparison of the pair emission spectra obtained by positron, electron and photon excitation. Higher resolution measurements of the (e^+,e^+e^-) spectrum from LiF(1 0 0) are planned and model calculations are underway.

Acknowledgments

We gratefully acknowledge the support from Dr. C. Hugenschmidt, J. Mayer, P. Pikart and C. Piochacz for their advice and assistance at NEPOMUC, and from Dr. W. Mahler and B. Zada at the UE56/2-PGM-1 beamline at BESSY II.

References

[1] Van Riessen G, Schumann F O, Birke M, Winkler C and Kirschner J 2008 *J. Phys.: Condens. Matt.* **20** 442001
[2] Ortiz G, Souza I and Martin R M 1998 *Phys. Rev. Lett.* **80** 353
[3] Nekovee M, Foulkes W M C and Needs R J 2001 *Phys. Rev. Lett.* **87** 036401
[4] Perdew J P, Burke K and Wang Y 1996 *Phys. Rev. B* **54** 16533
[5] Schumann F O, Kirschner J and Berakdar J 2005 *Phys. Rev. Lett.* **95** 117601
[6] Schumann F O, Winkler C and Kirschner J 2007 *New J. Phys.* **9** 372
[7] Schumann F O, Winkler C and Kirschner J 2007 *Phys. Rev. Lett.* **98** 257604
[8] Samarin S, Artamonov O M, Suvorova A A, Sergeant A D and Williams J F 2004 *Sol. Stat. Commun.* **129** 389
[9] Feder R, Gollisch H, Meinert D, Scheunemann T, Artamonov O M, Samarin S N and Kirschner J 1998 *Phys. Rev. B* **58** 16418–16431
[10] Berakdar J 1998 *Phys. Rev. B* **58** 9808
[11] Fominykh N, Henk J, Berakdar J, Bruno P, Gollisch H and Feder R 2000 *Sol. Stat. Commun.* **113** 665
[12] Gollisch H, v Schwartzenberg N and Feder R 2006 *Phys. Rev. B* **74** 075407
[13] Puska M J and Nieminen R M 1994 *Rev. Mod. Phys.* **66** 841
[14] Stachowiak H and Boroński E 2005 *Phys. Rev. B* **71** 245107

[15] Boroński E and Stachowiak H 2005 *Physica B: Cond. Matt.* **366** 168
[16] Mills A P and Crane W S 1985 *Phys. Rev. B* **31** 3988
[17] Berakdar J 2000 *Nucl. Inst. Meth. Phys. Res. B* **171** 204
[18] Giebels F, Gollisch H and Feder R 2009 *J. Phys. Condens. Matt.* **21** 355002
[19] Herrmann R, Samarin S, Schwabe H and Kirschner J 1998 *Phys. Rev. Lett.* **81** 2148
[20] Hattass M, Jahnke T, Schossler S, Czasch A, Schoffler M, Schmidt L P H, Ulrich B, Jagutzki O, Schumann F O, Winkler C, Kirschner J, Dörner R and Schmidt-Böcking H 2008 *Phys. Rev. B* **77** 165432–9
[21] Muñoz-Navia M, Winkler C, R Patel M, Schumann F O and Kirschner J 2009 *J. Phys.: Condens. Matter* **21** 355003
[22] Hugenschmidt C, Schreckenbach K, Stadlbauer M and Strafler B 2005 *Nucl. Inst. Meth. Phys. Res. A* **554**
[23] Van Riessen G A, Schumann F O, Birke M, Winkler C and Kirschner J 2009 *Journal of Physics: Conference Series* **185** 012051
[24] Sawhney K, Senf F, Scheer M, Schäfers F, Bahrdt J, Gaupp A and Gudat W 1997 *Nucl. Instr. Meth. Phys. Res. A* **390** 395–402
[25] Fominykh N Unpublished results.
[26] Fominykh N, Berakdar J, Henk J and Bruno P 2002 *Phys. Rev. Lett.* **89** 086402

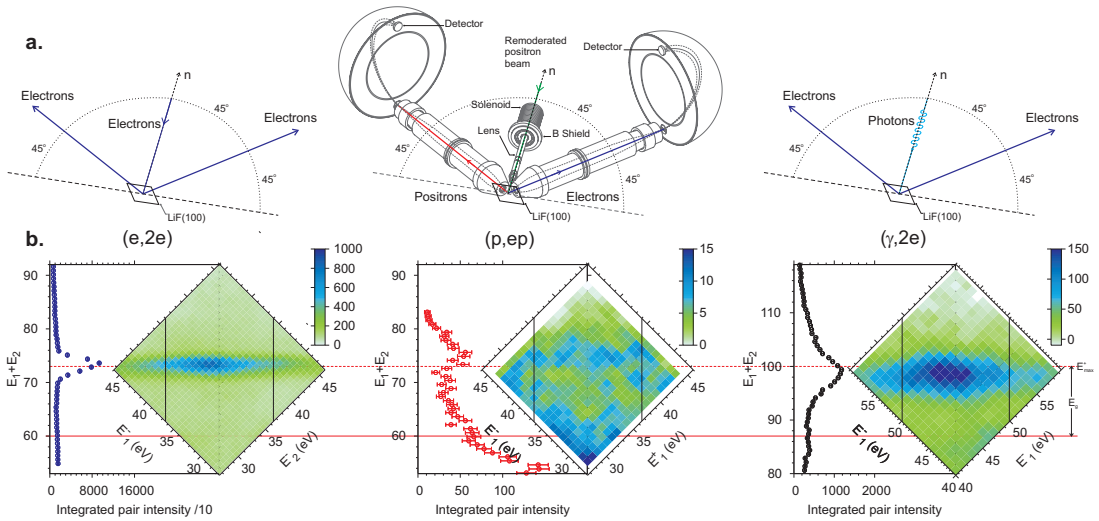

Figure 1. (a) The equivalent (symmetric coplanar) experimental geometry used with an electron, positron and photon excitation source. For the positron case a simplified diagram of the experimental apparatus is shown with the two hemispherical analyzers and the final stage of the positron optics. (b) The measured pair energy distributions are shown together with a projection of the data between the vertical lines onto the line $E_1 + E_2$, where E_1 and E_2 are the measured particle energies. Electron (positron) energies are indicated by a negative (positive) superscript.

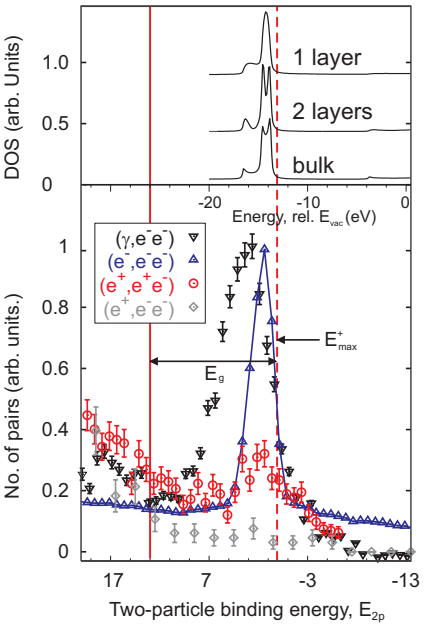

Figure 2. Two-particle binding energy distributions for (e^-,e^-e^-), (e^+,e^+e^-), and $(\gamma, 2e)$ measured from LiF(1 0 0), scaled for comparison. The distributions correspond to the projections onto the line $E_1 = E_2$ shown in Figure 1. For explanation of the energy scale, see text. In the upper panel the bulk and layer resolved DOS [25] is included for comparison.